Investigating the impact of $MASNBR_3$ absorbent layer thickness on $FTO/TiO_2/MASnBr_3/CuI$ perovskite solar cells characteristics

T. A. Mohammed[a], M. W. Aziz[a], H. W. Hamed[a], J. M. Rzaij[b,*]
[a]*Department of Physics, College of Education for Women, University of Kirkuk, Iraq*
[b]*Department of Physics, College of Science, University of Anbar, Ramadi, Iraq*

This work involved designing a solar cell with layers of fluorine-doped tin oxide, titanium dioxide, methylammonium tin bromide, and cuprous iodide. The impact of absorbent layer thicknesses ranging from 0.2 µm to 2.5 µm on developed PSC properties was examined. The thickness of the absorption layer that performs the optimally is discovered to be 0.2 µm. The synthetic solar cell provided an open circuit voltage of 1.07 V, a short circuit current of 34.356 mA/cm^2, an efficiency of 30.68%, and a fill factor of 83.404 at an optimal thickness of 0.2 µm. The findings proved the developed PSC's cost-effectiveness, increased environmental sustainability, and robustness compared to traditional counterparts.

(Received February 16, 2024; Accepted May 3, 2024)

Keywords: Perovskite, Solar cells, SCAPS-1D, Efficiency, Fill factor, Quantum efficiency

1. Introduction

The Earth receives an immense amount of solar energy, with the sun providing in a single minute enough energy to satisfy the global energy demand for an entire year. Furthermore, each day's solar radiation exceeds the total energy consumption of the world's population. The solar energy reaching the Earth for three days is equivalent to the energy stored in all known fossil fuel sources. Solar energy, being freely available, represents a promising and sustainable resource. The inception of practical solar cell technology dates back over 30 years. The efficiency and longevity of solar cells have notably improved over time, particularly with advancements in transistor and semiconductor technology. Photovoltaic technology, which converts light energy into electrical current, stands out as one of the most prospective forms of renewable energy globally [1–3].

Solar cells function by converting light, whether from sunlight or artificial sources, into electrical energy. Ongoing developments aim to produce cost-effective, user-friendly, highly efficient, and durable solar cells, commonly referred to as stable solar cells. Perovskite solar cells, a category of solar cells featuring a perovskite-structured compound, have garnered attention. This compound, often an organic-inorganic hybrid or predominantly lead-based halide material, serves as the active layer for energy collection. Noteworthy perovskite materials include lead methyl ammonium and lead cesium halides, known for their cost-effectiveness and simplicity in manufacturing. Advancements in perovskite solar cell technology have seen a significant increase in efficiency, rising from 3.8% in 2009 to 22.7% in late 2018 [4], attributed to internal structural modifications. Explorations into non-lead alternatives have led to the investigation of metal halides such as Sb, Ag, Sn, Cu, Ge, and Bi in the creation of perovskite solar cells. Specifically, perovskites containing metal halides, such as $CH_3NH_3SnBr_3$, have emerged as promising candidates for non-lead perovskite solar cells due to their ideal band gap of 1.3 eV. These developments underscore the potential for sustainable and efficient solar energy technologies as we strive to transition towards cleaner and more renewable energy sources [5].

Park et al. successfully developed this cell in 2011, employing the same principle, and achieved an energy conversion efficiency of 6.5% [6]. In 2017, *Anwar et al.* studied a solar cell with a multi-type perovskite absorption layer, and they found an efficiency of 20.21%, 20.23%, and 18.34% [7]. In 2018, *Muniandy et al.* designed a perovskite solar cell using different types of

* Corresponding author: sc.jam72al@uoanbar.edu.iq
https://doi.org/10.15251/DJNB.2024.192.707

absorption layers, including $MASnBr_3$, and they obtained an efficient 9.58% [8]. *Mohammed* studied the thickness and reflectivity of the perovskite solar cell in 2019. The obtained efficiency of PSC was 20.98% [4]. *Husainat et al.* studied in 2019 a solar cell using a methylammonium lead iodide ($CH_3NH_3PbI_3$) absorption layer, and initial results showed a power conversion efficiency of 20.34% [9]. This study highlights that the prepared cell is toxic due to its lead content and lower efficiency when compared to the lead-free, higher-efficiency solar cell developed in our current work. In 2020, *Husainat et al.* investigated a progressive PSC, they identified the impact of the material used for absorption and contact on the absorption material's effectiveness. The MBMT-MAPLE/PLD program was adopted as a method for creating a special simulation program, and efficiencies were obtained: 27.25%, 26.52%, 18.90%, 25.66%, and 22.77% [10]. *Islam et al.* modeled a system for perovskite solar cells and used $CH_3NH_3SnBr_3$. As an absorber for perovskite, an efficiency of 21.66% was obtained in 2021[11]. In 2022, *Munef et al.* studied the effect of changing the thickness of the solar cell and were able to obtain an efficiency of 17.46% [12]. *Kumavat* in 2023 studied the perovskite solar cell and added light harvesting materials, the obtained efficiency was 23.46% [13]. The main objective of this work was to achieve high perovskite solar cell performance efficiency and reduce the absorbent layer thickness, reducing the manufacturing cost compared to the previously manufactured cell. Moreover, this work also focused on developing an environmentally friendly solar cell, unlike the earlier cells that relied on lead, improving the cell's lifespan and enhancing its efficiency in various environmental conditions. So, this study showcases the advantages of the improved solar cell in terms of cost savings, environmentally friendly, and enhanced durability compared to traditional solar cells.

2. Key factors characterized solar cell performance

Solar cell performance is characterized by key factors such as short-circuit current density (J_{sc}), open circuit voltage (V_{oc}), fill factor (FF), conversion efficiency (η), quantum efficiency (QE). Below is a concise explanation of these factors and the mathematical calculations employed to determine them.

2.1. Short circuit current density (J_{sc})

Short circuit current density (J_{sc}) refers to the greatest electrical current generated by a solar cell when its terminals are directly linked, resulting in a short circuit. it is obtained from the total current density $J(V)$ solar system using the Equation (1) [14].

$$J(\mathrm{V}) = J_{sc} - J_{dark} \tag{1}$$

where: J_{dark} is the density of the dark current and is given by Equation (2).

$$J_{dark}(\mathrm{V}) = J_0\left(e^{qv/k_BT} - 1\right) \tag{2}$$

Under solar illumination, the behavior of a solar cell is explained using the ideal diode equation (Equation 2) along with an extra current source (J_{sc}) attributed to the illumination. So, the total current density of the solar cell is given by Equation 3.

$$J(\mathrm{V}) = Jsc - J_0\left(e^{qv/k_BT} - 1\right) \tag{3}$$

Similarly, the equation below provides the short circuit current:

$$Jsc(\mathrm{V}) = J(\mathrm{V}) + J_0\left(e^{qv/k_BT} - 1\right) \tag{4},$$

since v is the voltage across the junction, T is the absolute temperature. J_0 is the density of the saturation dark current.

2.2. Voltage open circuit (V_{oc})

Voltage open circuit is the voltage at which no current flows when the solar cell terminals are not connected, and calculated by using the equation (5) by adjusting the net current $J(\mathrm{V})$ to zero [14]:

$$V_{oc} = \frac{K_B T}{q} ln\left(\frac{J_{ph}}{J_0} + 1\right) \tag{5}$$

2.3. Fill factor (FF)

The fill factor is defined by the ratio of the maximum power produced to the product of the open-circuit voltage and short-circuit current, as expressed by Equation (6):

$$FF = \frac{J_{mp} \times V_{mp}}{V_{oc} J_{sc}} = \frac{P_{max}}{V_{oc} J_{sc}} \tag{6}$$

J_{mp} and V_{mp} represent the solar cell's highest current density and voltage, respectively.

2.4. Conversion efficiency (η)

The conversion efficiency of a solar cell is defined as the ratio of the maximum power solar cell to the incident power. Mathematically, it can be expressed using Equation (7).

$$\eta = \frac{P_{max}}{P_{in}} = \frac{J_{sc} V_{oc}\, FF}{P_{in}} \tag{7}$$

P_{in} is a standard for the conversion efficiency of a solar cell and represents the power incident on the solar cell, which depends on the area of the cell. In this study, P_{in} was 1000 W/m^2 from the 1.5 AM spectrum, which is the sunlight located at an angle of 48.2° from the zenith point at 25 °C [15].

2.5. Quantum efficiency (Q_E)

Quantum efficiency is the ratio of the number of generated electrons to the number of photons absorbed per unit wavelength incident on the surface of the device and is expressed by Equation (8).

$$Q_E = \frac{I_{ph}/q}{P_{in}/hv} \tag{8},$$

where I_{ph}/q is the number of carriers generated and P_{in}/hv is the number of incident photons. Also Q_E can also be expressed in terms of wavelength and responsivity (R_λ), in terms of Equation (9).

$$Q_E = R_\lambda \frac{hc}{q\lambda} \tag{9}$$

Since $\frac{hc}{q}$ is a constant (1.24), the Equation (9) can be written as:

$$Q_E = 1.24 \frac{R_\lambda}{\lambda} \tag{10}$$

These parameters collectively provide a comprehensive understanding of the solar cell's performance under various conditions and facilitate evaluating and optimizing its efficiency.

3. Solar cell configuration

Perovskite material structure is a crystalline material characterized by the formula ABX3. Specifically, A stands for a large organic or inorganic cation, B denotes a smaller inorganic cation (e.g., $Cu^{2+,}$ $Sn^{2+,}$ Pb^{2+}), and X is an ion from the halogen group (e.g., Cl^{-}, Br^{-}or I^{-}). This structure enables bonding with both cations A and B. Fig (1) illustrates the crystal structure of Perovskite [9]. The configuration of a solar cell based on Perovskite involves utilizing this unique material structure to harness photovoltaic capabilities. The A, B, and X elements in Perovskite contribute to its electronic properties, making it a promising candidate for solar cell applications. Understanding the crystal structure is crucial for optimizing the design and performance of Perovskite solar cells, enabling advancements in renewable energy technologies. In a broader context, the solar cell is comprised of several key components, including a thin TiO_2 buffer layer placed purposefully between the absorbent layer ($MASnBr_3$) layer and the FTO front contact layer to reduce surface recombination and a CuI back contact layer deposited on the $MASnBr_3$ to address the non-ohmic back contact that the absorption layer faces.

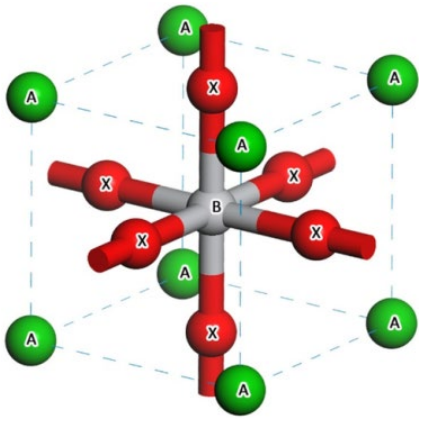

Fig. 1. The structure of the perovskite.

To ensure that photons can pass through it, the FTO layer comprises doped N-type semiconductors with an energy gap larger than the absorption layer to enhance the radiation influence passing through it [16]. Finally, a 95% mirror filter from the default library of SCAPS-1D was used as the final layer. Fig. 2 depicts the structure of the simulated solar cell, with the $MASnBr_3$ absorbent layer being the critical component in this configuration. The solar cell layers' characteristics for TiO_2/FTO/i-$MASnBr_3$/CuI are listed in Table 1 and Table 2.

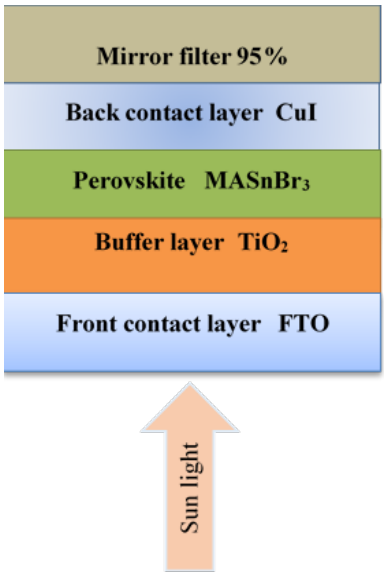

Fig. 2. The structure of the simulated solar cell.

Table 1. TiO_2/FTO/i-$MASnBr_3$/CuI solar cell data used in the SCAPS-1D simulation program.

Parameters	**Symbol (unit)**	**TiO_2**	**FTO**	**$MASnBr_3$**	**CuI**
Thickness	d (μm)	0.5	0.5	variable	0.5
Energy gap	Eg (eV)	3.26	4.2	1.3	3.4
Electron affinity	X (eV)	4.2	4.5	4.17	2.1
Dielectric permittivity	D_k	10	10	10	10
Density of state in CB	$Nc(cm^{-3})\times10^{18}$	2.2	120	2.2	2.5
Density of state in VB	$Nv\ (cm^{-3})\times10^{20}$	0.18	7	0.18	0.18
Thermal Speed of Electron	V_{th} (cm/s)$\times10^7$	1	1	1	1
Thermal Speed of Holes	V_{th} (cm/s))$\times10^7$	1	1	1	1
Electron mobility	$\mu_n\ (cm^2/Vs)\times10^2$	1	0.2	0.016	200
Hole mobility	$\mu_p\ (cm^2/Vs)\times10^2$	0.25	1	0.016	200
Donor concentration	$N_d\ (cm^{-3})\times10^{15}$	100	10	1	-
Acceptor concentration	$N_a\ (cm^{-3})\times10^{15}$	-	-	1	10^5

Table 2. Defect parameters of the solar cell layers.

Parameters	**TiO_2**	**FTO**	**$MASnBr_3$**	**CuI**
Defect type	Single donor (0/+)	Single donor (0/+)	Neutral	Neutral
Cross Section-capture electron (cm^2)	10^{-17}	10^{-15}	10^{-15}	10^{-15}
Cross Section-capture holes (cm^2)	10^{-15}	10^{-12}	10^{-15}	10^{-15}
Distribution of Energy	individual	individual	individual	individual
Defect energy level reference Et	Over eV	Over eV	Over eV	Over eV
Reference energy level (eV)	0.600	0.600	0.600	0.600

The thicknesses of the front contact layer (window), buffer layer, and back contact layer were all adjusted to 0.5 μm. The thickness of the absorption layer ($MASnBr_3$) has been varied between 0.2 μm and 2.5 μm to investigate the impact of the absorption layer on the efficiency of the TiO_2/FTO/$MASnBr_3$/CuI solar cell.

4. Results and discussion

The Jsc-V characteristic curve of the TiO_2/FTO/$MASnBr_3$/CuI solar cell is examined within a voltage range of 0V to 1V, as depicted in Figure 3. The depicted figure demonstrates a positive correlation between the J_{SC}-V curve and the thickness of the absorption layer. Figure 3

revealed a significant increase in current at 0.8 V, indicating the efficient generation of electron-hole pairs [17,18].

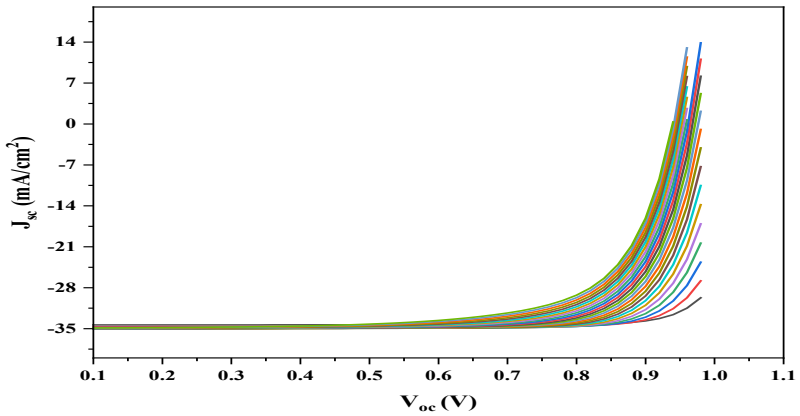

Fig. 3. I-V characteristic curve of the TiO_2/FTO/$MASnBr_3$ /CuI solar cell.

Fig. 4a shows the effect of $MASnBr_3$ thickness on the short circuit current density (J_{sc}). When the thickness of the absorbent layer is increased from 0.2 to 1.2 µm, the J_{sc} increases from 34.35 to 34.99 mA/cm^2, and after that, it decreases to 34.91 mA/cm^2 when the thickness reaches 2.5 µm. The material's enhanced photon absorption increases the production of electron-hole pairs, increasing the short-circuit current. In contrast, the decline in the short circuit current is attributed to surface recombination [19], resulting in electron depletions and reducing the short circuit current density [7,20].

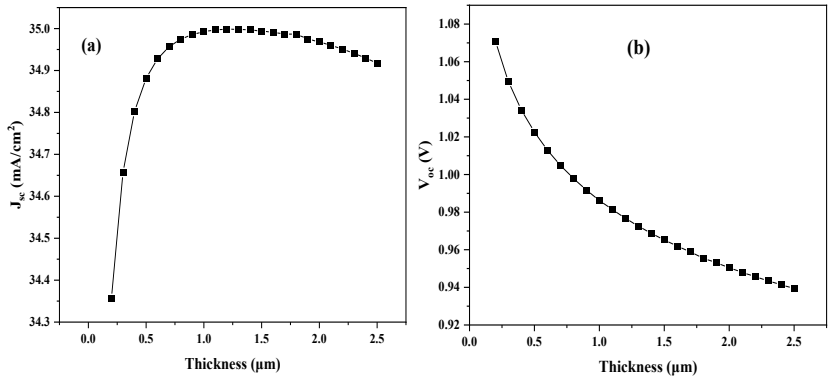

Fig. 4. $MASnBr_3$ thickness varying impact on (a) short circuit current density and (b) open circuit voltage.

Furthermore, as illustrated in Fig. 4b, the open circuit voltage exhibited a distinct behavior compared to the short circuit current density. Specifically, it reduced from 1.070 volts to 0.939 volts when the thickness was varied from 0.2 µm to 2.5 µm. This behavior is ascribed to parallel resistance.

The analysis of the fill factor (FF) demonstrated a decline as the thickness of the absorption layer increased, dropping from 83.40 at a thickness of 0.2 µm to 71.81 at 2.5 µm, as depicted in Fig. 5a. The filling factor decreases with increasing absorbent layer thickness, which can be explained as follows: The filling factor is negatively impacted by the increased contact between the surfaces, which forms traps, supporting the capture of electrons and resulting in a drop in current. Moreover, series resistance also affects the filling factor; as the absorption layer thickness increases, series resistance likewise rises and lowers the filling factor [21]. An additional aspect investigated in this study is the determination of the solar cell's conversion efficiency (η) with the thickness varying of the absorbing layer, as illustrated in Fig.5b. It was discovered that the

efficiency of the solar cell decreased as the thickness of the absorbent layer increased. This is due to an increase in the recombination rate with increasing thickness, which leads to a decrease in the efficiency of the solar cell [22–24]. Table 3 displays the results obtained from investigating the effect of the $MASnBr_3$ thickness absorbent layer on the characteristics of the analyzed TiO_2/FTO/$MASnBr_3$/CuI solar cell.

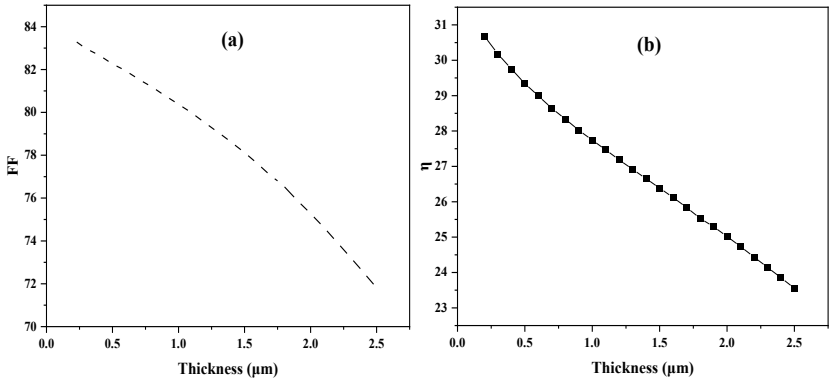

Fig. 5. Absorbent thickness variation effect on (a) fill factor and (b) conversion efficiency.

Table 3. Results of the effect of absorbent layer thickness.

Thickness (µm)	V_{oc} (V)	J_{sc} mA/cm^2	FF	η
0.2	1.070716	34.3562	83.4041	30.6808
0.3	1.049349	34.65699	82.9804	30.1777
0.4	1.03	34.80209	82.6603	29.7527
0.5	1.022609	34.88147	82.2643	29.3437
0.6	1.012952	34.92814	81.9421	28.9915
0.7	1.004919	34.95674	81.5369	28.6428
0.8	0.997965	34.97464	81.1839	28.336
0.9	0.991711	34.9858	80.7689	28.0234
1	0.986243	34.99249	80.3821	27.7407
1.1	0.98137	34.99698	79.9756	27.4676
1.2	0.976782	34.99848	79.5139	27.1825
1.3	0.97257	34.99825	79.0725	26.9149
1.4	0.968739	34.99667	78.6093	26.6506
1.5	0.965222	34.99395	78.1215	26.387
1.6	0.961968	34.9913	77.6031	26.1216
1.7	0.958866	34.98676	77.0246	25.8399
1.8	0.958866	34.98676	77.0246	25.8399
1.9	0.953078	34.97513	75.885	25.2955
2	0.950465	34.96801	75.2758	25.0186
2.1	0.948008	34.96002	74.6362	24.7362
2.2	0.945689	34.95104	73.9381	24.4386
2.3	0.94349	34.94101	73.249	24.1476
2.4	0.941397	34.9298	72.5385	23.8527
2.5	0.939363	34.91728	71.8101	23.5537

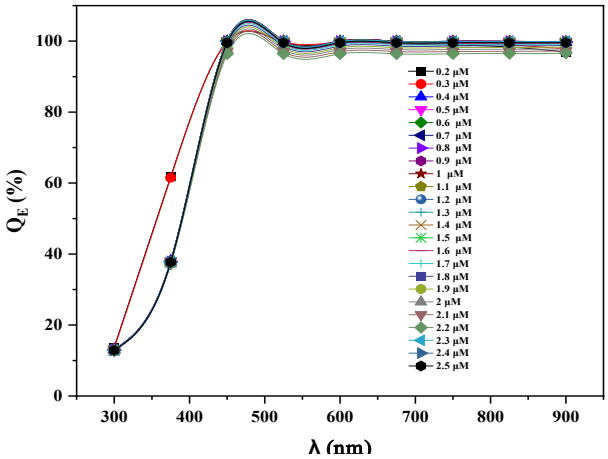

Fig. 8. Q_E (%) with wavelength at different thickness variation.

The quantum efficiency ($\eta\%$) of the simulated solar cell as a function of the wavelength is displayed in Fig. 8. The η% of the simulated solar cell rises as the thickness of the absorber layer grows, up to a wavelength of 500 nm. This is due to the increased absorption of photons by the absorber layer, leading to the generation of more electron-hole pairs. The decrease in quantum efficiency beyond 500 nm wavelengths resulted from a decrease in the absorption coefficient. This led to a decline in the rate of carrier generation and a loss in the rate of recombination at the back surface of the cell. Consequently, the carrier propagation length was reduced, ultimately resulting in a decrease in the number of electrons produced for each absorbed photon, as described by Equation (10) [23,25].

5. Conclusion

The present study addresses the design of a perovskite solar cell by utilizing computer modeling tools. The findings indicated that increasing the thickness of the absorbent layer, as suggested in this study, significantly influenced the open circuit voltage and fill factor, thus impacting the efficiency of the solar cell. The absorbent layer's optimal thickness was 0.2 µm, resulting in a maximum quantum efficiency of 30.68%. The efficiency of the simulated cell reduced to 23.55% as the thickness of the absorbent layer increased to 2.5 µm. Therefore, it can be inferred that the suggested solar cell has practical applicability and shows promising results, which will aid in lowering the design costs.

References

[1] H. Fang, X. Li, S. Song, Y. Xu, J. Zhu, Nanotechnology 19(25), 255703 (2008); https://doi.org/10.1088/0957-4484/19/25/255703

[2] I. M. Ibrahim, J. M. Rzaij, A. Ramizy, Digest Journal of Nanomaterials and Biostructures 12(4), 1187 (2017).

[3] J. M. Rzaij, N. F. Habubi, Journal of Materials Science: Materials in Electronics 33(15), 11851 (2022); https://doi.org/10.1007/s10854-022-08148-2

[4] A. Babayigit, H.-G. Boyen, B. Conings, MRS Energy & Sustainability 5(1), 15 (2018); https://doi.org/10.1557/mre.2017.17

[5] J.-H. Im, C.-R. Lee, J.-W. Lee, S.-W. Park, N.-G. Park, Nanoscale 3(10), 4088 (2011); https://doi.org/10.1039/c1nr10867k

[6] Tariq A. Mohammed, Ayed N. Saleh, Tikrit Journal of Pure Science 24(7), 93 (2019); https://doi.org/10.25130/j.v24i7.917

[7] F. Anwar, R. Mahbub, S. S. Satter, S. M. Ullah, International Journal of Photoenergy 2017, 1 (2017); https://doi.org/10.1155/2017/9846310

[8] S. Muniandy, M. I. Bin Idris, Z. A. F. Bin Mohammed Napiah, H. H. Mohd Yusof, S. A. Mohd Chachuli, M. Rashid, 2021 IEEE Regional Symposium on Micro and Nanoelectronics (RSM) (IEEE, 2021), pp. 112-115; https://doi.org/10.1109/RSM52397.2021.9511573

[9] A. Husainat, W. Ali, P. Cofie, J. Attia, J. Fuller, American Journal of Optics and Photonics 7(2), 33 (2019); https://doi.org/10.11648/j.ajop.20190702.12

[10] A. Husainat, W. Ali, P. Cofie, J. Attia, J. Fuller, A. Darwish, American Journal of Optics and Photonics 8(1), 6 (2020); https://doi.org/10.11648/j.ajop.20200801.12

[11] M. Samiul Islam, K. Sobayel, A. Al-Kahtani, M. A. Islam, G. Muhammad, N. Amin, M. Shahiduzzaman, M. Akhtaruzzaman, Nanomaterials 11(5), 1218 (2021); https://doi.org/10.3390/nano11051218

[12] R. A. Munef, M. M. Ameen, R. B. Abdulrahman, H. Waleed, A. M. Ghelab, NeuroQuantology 20(2), 69 (2022); https://doi.org/10.14704/nq.2022.20.2.NQ22027

[13] S. R. Kumavat, Y. Sonvane, RSC Advances 13(12), 7939 (2023); https://doi.org/10.1039/D3RA00108C

[14] M. Ahemad, M. Kibret, Journal of King Saud University - Science 26(1), 1 (2014); https://doi.org/10.1016/j.jksus.2013.05.001

[15] K. Ranabhat, L. Patrikeev, A. Antal'evna-Revina, K. Andrianov, V. Lapshinsky, E. Sofronova, Istrazivanja i projektovanja za privredu 14(4), 481 (2016); https://doi.org/10.5937/jaes14-10879

[16] J. M. Rzaij, Q. A. Abbas, A. M. Khalaf, Bulletin of Materials Science 46(4), 200 (2023); https://doi.org/10.1007/s12034-023-03040-z

[17] O. S. Shawki, J. M. Rzaij, (AIP Conference Proceedings, 2023), (March), p. 020009; https://doi.org/10.1063/5.0112172

[18] M. Muzammil, K. Naik Naam, M. Fareed, M. Shafaat Hussain, M. Zulfiqar, Chemical Physics Impact 8, 100407 (2024); https://doi.org/10.1016/j.chphi.2023.100407

[19] A. S. Ibraheam, J. M. Rzaij, M. K. M. Arshad, Journal of Electronic Materials 52(1), 414 (2023); https://doi.org/10.1007/s11664-022-10002-4

[20] J. Correa-Baena, M. Anaya, G. Lozano, W. Tress, K. Domanski, M. Saliba, T. Matsui, T. J. Jacobsson, M. E. Calvo, A. Abate, M. Grätzel, H. Míguez, A. Hagfeldt, Advanced Materials 28(25), 5031 (2016); https://doi.org/10.1002/adma.201600624

[21] H. Dixit, D. Punetha, S. K. Pandey, Optik 179, 969 (2019); https://doi.org/10.1016/j.ijleo.2018.11.028

[22] B. Mohammed, College Of Basic Education Research Journal 17(2), 1571 (2021); https://doi.org/10.33899/berj.2021.168558

[23] M. I. Saidaminov, A. L. Abdelhady, B. Murali, E. Alarousu, V. M. Burlakov, W. Peng, I. Dursun, L. Wang, Y. He, G. Maculan, A. Goriely, T. Wu, O. F. Mohammed, O. M. Bakr, Nature Communications 6(1), 7586 (2015); https://doi.org/10.1038/ncomms8586

[24] M. Yuan, O. Voznyy, D. Zhitomirsky, P. Kanjanaboos, E. H. Sargent, Advanced Materials 27(5), 917 (2015); https://doi.org/10.1002/adma.201404411

[25] P. Lin, L. Lin, J. Yu, S. Cheng, P. Lu, Q. Zheng, Journal of Applied Science and Engineering 17(4), 383 (2014).